

Numerical Studies of Melting Process Employing Nano-enhanced Phase Change Materials for Two-dimensional Rectangular and Circular Geometries

Neha Gautam^{1,*}, Kundan Kumar¹, and Achintya Kumar Pramanick¹

¹Department of Mechanical Engineering, National Institute of Technology Durgapur, India

Abstract

In this present article the numerical studies of melting process by applying nano-enhanced phase change materials for energy storage in different two-dimensional geometries like rectangular and as well as circular cavities are reported. The basic phase change material employed is paraffin wax and subsequently the nano-enhancement was achieved through the addition of alumina at different percentages. ANSYS-FLUENT commercial software was used. The results presented are grid independent. The results obtained are compared with the results obtained from three-dimensional geometry in base cases available in literature. It is observed that rectangular geometry performs better in terms of melting and subsequently for heat storage. Nano materials are further helpful for the betterment of system performance in terms of melting.

Keywords: PCM, paraffin wax, nano enhanced paraffin wax, Latent heat storage, Alumina (Al_2O_3)

1. Introduction

Organic Phase Change Materials (PCM) is plentifully practiced as energy storage material due to the scanty of natural energy sources. There is a requirement of a proper backup to combat the global warming contagious effect. Waste heat recovers from various energy devices can be stored easily in PCM through melting and can be used again when required through the process of solidification. Based on temperature range PCM energy storage devices are classified [1]. If the temperature is below 15°C PCM storage device is used to store coldness in air cooling devices and for temperature greater than 90°C it employed as absorbing refrigerator device. Further for temperature range between 15°C and 90°C it is used as solar heating and during off-peak hours for power management. Density varies with the solidification and melting process as it is concluded by various experimental studies that there is a change of 10% in the volume during charging and discharging processes. To avoid this difficulty some space should be given in a PCM storage device for proper solidification and melting. In nature, a large variety of PCM material is available each variety of PCM has its own pros and cons.

PCM is available in both organic and inorganic form in nature for which authors [2-3] made a comparative observations among available PCM materials. Paraffin wax is suitable for the energy storage devices compared to other organic PCM

materials. Paraffin wax is non-toxic, chemically stable, nonflammable, store energy at the low-temperature range, easily available at low cost, desirable latent heat storage capacity, and improved density. However natural PCM has lower thermal conductivity in contradiction of inorganic PCM. Rigorous efforts are made by researchers to improve the poor thermal conductivity of Paraffin wax material and a lot of research is still needed in this direction [7-8].

In the present article a numerical study of paraffin wax is done for the heat storage device. For improvement in the thermal conductivity of wax, alumina (Al_2O_3) is used as a nanoparticle. Alumina is an inexpensive nanoparticle and used by various researchers for experimental studies [9]. Performance investigation of organic phase change material paraffin wax embedded with alumina nanoparticle for latent heat energy storage system in a double pipe concentric heat exchanger is done for the same time and the increment in melting rate as compared to base material was observed 12.3%, 10.6%, 15.4% respectively, for 2%, 5% and 10% alumina in paraffin wax. For solidification process the amount of energy storage was improved by 25.6%, 31.8%, and 41.8% respectively, for 2%, 5% and 10% alumina in paraffin wax. Improvement in thermal conductivity and other properties of wax is observed with 2%, 5%, and 10% of a nanoparticle [10]. Nanoparticle does not increase the cost too much and also not create the problem of phase separation due to their presence in a very small amount.

PCM has applications [4-6] in wide range of industries such as space application, solar cooling, solar power plant, electronic cooling devices, waste heat recovery system, fiber industry, solar dryer in agriculture industry, domestic hot water, pharmaceutical products and food storage, among a host. Various energy storage devices can be installed at enduring conventional plants for significant improvement in the efficiency.

2. Physical Model

In the present research work comparison between two different 2-dimensional geometries having the same area is carried out and constant heat flux boundary condition is applied on both the geometries. Heat flux rate is kept constant for both cases. The melting rate of PCM material is observed for both cases and nanoparticle alumina is employed for the geometry with a better melting rate. Here, the first geometry [11] as depicted in Fig. 1(a) is taken as a rectangular cavity (150mm×100mm). In another case as shown in Fig.1(b) it is a

circular cavity of radius 69.10mm. Numerical study of two cases is done first with paraffin wax and second with nano-paraffin wax with alumina at volume percentages of 2%, 5%, and 10%. The initial temperature of PCM is considered as 300K.

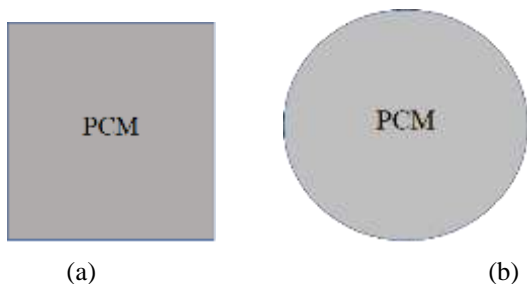


Fig. 1 Heat flux (2500 W/m^2) from all sides– (a) rectangular cavity, (b) circular cavity.

Following assumptions are made for further numerical analysis:

1. Newtonian and incompressible fluid.
2. Flow in the melting region is laminar and has negligible viscous dissipation.
3. Temperature-dependent physical properties are considered.
4. Both conduction and convection modes of heat transfer is considered.
5. Volumetric variation due to phase change has been neglected.
6. A 2-dimensional model is used for the present numerical analysis.

Detailed analysis for charging process of phase change material along with mixture of nanoparticle has been done inside a square cylinder using both experimental and numerical techniques that is subjected to constant heat flux boundary condition [12].

3. Computational Methodology

2-dimensional computational analysis of both models has been conducted using CFD programming software ANSYS-FLUENT (Version 17.1). The design modeler of Ansys 17.1 was utilized in the demonstrating of 2-dimensional calculation for a rectangular and circular computational domain both. It has been reported that results obtained by the analysis made for the 2-dimensional domain are in good agreement with the 3-dimensional domain as reported in the literature [13]. For this reason in the current analysis 2-dimensional model was selected as a matter of model reduction.

3.1 Mesh generation and grid independency test:

ANSYS (v17.1) meshing module was actualized in the model to generate non uniform structured mesh generation as shown in Fig. 2.

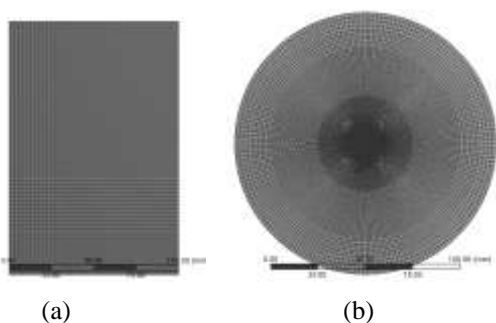


Fig. 2 Grid for present computational analysis: (a) rectangular cavity, (b) circular cavity.

Finer grid size was created near the walls to capture more precise result near the wall in rectangular geometry while in circular geometry finer grid size was created near the center. Grid independency test has been conducted for both the geometries to make the result free of grid size as shown in Fig. 3. In this present study seven mesh elements were considered viz., 600, 1700, 6700, 8932, 10500, 12467, and 15000 for rectangular geometry and 2792, 6257, 11142, 15773, 24702, 44248, and 99048 for circular geometry. All seven mesh elements were used to plot liquid fraction against number of elements for both the geometries as shown in the Fig. 3 and Fig. 4, respectively.

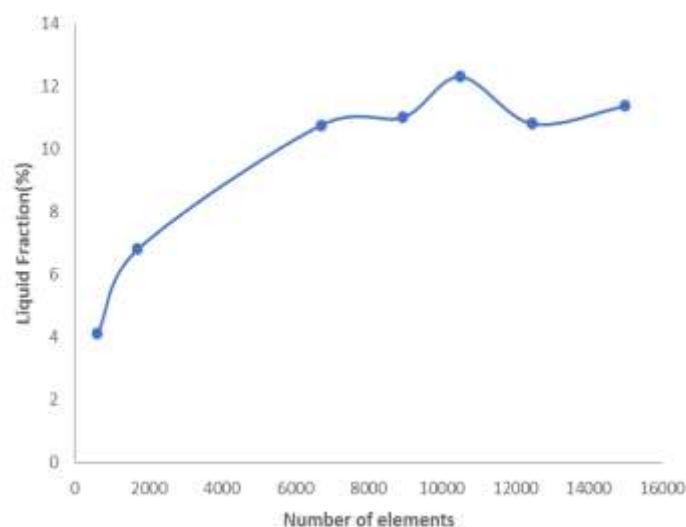


Fig. 3 Grid independency test for rectangular cavity.

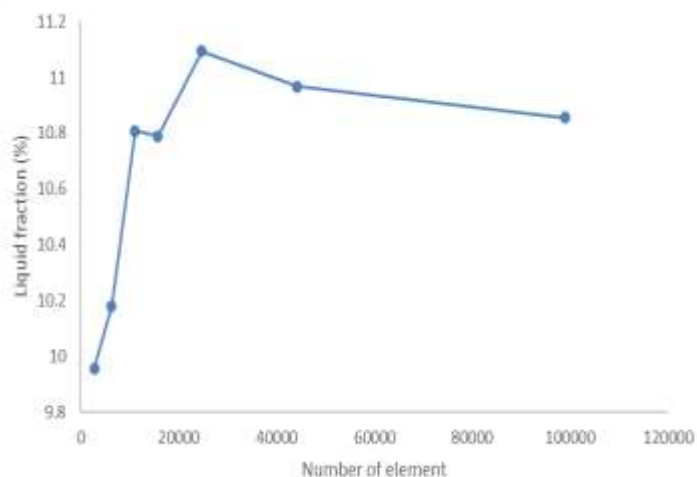


Fig. 4 Grid independency test for circular cavity.

It can be observed from the Fig. 3 and Fig. 4 respectively, that mesh elements 10500 for rectangular cavity and 24702 for circular cavity are the most optimum with respect to both accuracy and computational time.

Validation of following numerical model is performed with reference to the results that is available in literature [11] for rectangular cavity with constant heat flux applied from

verticle left side and remaining three walls are maintained at adiabatic wall conditions. A good agreement is observed between our work and the reference results [11]. The agreement is graphically presented in the Fig. 5.

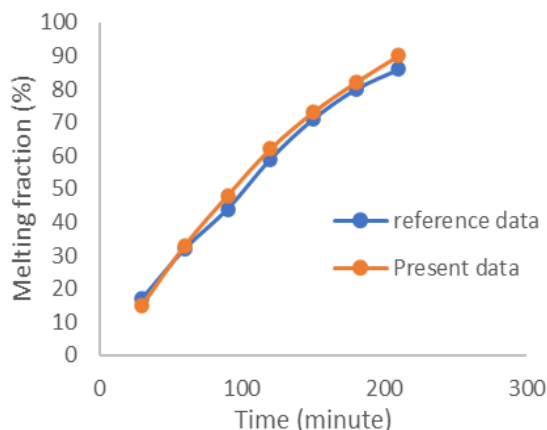


Fig. 5 Validation of rectangular cavity uniflux system with available data.

3.2 Governing equations

The continuity equation, momentum equation, and the energy equation for the solidification and melting can be written as follows:

Continuity equation:

$$\frac{\partial \rho}{\partial t} + \Delta(\rho \vec{U}) = 0, \quad (1)$$

Momentum equation:

$$\frac{\partial}{\partial t}(\rho \vec{U}) + \Delta(\rho \vec{U} \vec{U}) = -\Delta P + \rho \vec{g} + \Delta \vec{\tau} + \vec{F} \quad (2)$$

where P is the static pressure, $\vec{\tau}$ is the stress tensor, and $\rho \vec{g}$ and \vec{F} are the gravitational body force and external body forces, respectively.

Energy equation:

$$\frac{\partial(\rho H)}{\partial t} + \Delta(\rho \vec{U} H) = \Delta(K \Delta T) + S \quad (3)$$

Here H indicates the enthalpy of nePCM, temperature represents by symbol T . Density of nePCM symbolized by ρ , thermal conductivity of nePCM represents by K and the velocity represents using letter \vec{U} . Volumetric heat source of generation (S) assumed to be zero in present analysis. Overall enthalpy (H) of the nePCM is shown in term of summation of sensible enthalpy (h) and latent heat (ΔH).

$$H = h + \Delta H \quad (4)$$

where

$$h = h_{ref} + \int_{T_{ref}}^T c_p dT \quad (5)$$

Latent heat content in terms of L is represented as:

$$\Delta H = \beta L$$

β is the liquid fraction and it is defined in [14] as:

$$\beta = 0 \quad \text{if } T < T_{solidus} \quad (6)$$

$$\beta = 1 \quad \text{if } T > T_{liquidus} \quad (7)$$

$$\beta = \frac{T - T_{solidus}}{T_{liquidus} - T_{solidus}} \quad \text{if } T_{solidus} < T < T_{liquidus} \quad (8)$$

Iteration between the liquid fraction equation (7), and energy equation (3) can be carried out by the help of temperature solution. Mushy region is treated as a porous medium for enthalpy porosity technique. The values of porosity in individually cell will be same as the liquid fraction in that cell. Porosity is equal to zero in fully solidified regions, which terminate the velocity in these regions.

4. Thermophysical properties

Thermophysical properties of paraffin wax and alumina are mentioned in Table 1. Density, specific heat, latent heat, and viscosity of nano-enhanced PCM (nePCM) are defined as follows [16]:

$$\rho_{npcm} = \phi \rho_{np} + (1 - \phi) \rho_{pcm} \quad (9)$$

$$c_{p,npcm} = \frac{\phi(\rho c_p)_{np} + (1 - \phi)(\rho c_p)_{pcm}}{\rho_{npcm}} \quad (10)$$

and

$$L_{npcm} = \frac{(1 - \phi)(\rho L)_{pcm}}{\rho_{npcm}} \quad (11)$$

Dynamic viscosity and thermal conductivity of nanoenhanced PCM (nePCM) is taken from the work [17] as:

$$\mu_{npcm} = 0.983 e^{(12.959\phi)} \mu_{pcm} \quad (12)$$

For the count of effective thermal conductivity of nano-PCM, impacts of molecule size, molecule volume fraction and temperature reliance just as properties of base PCM and the Brownian movement of molecule are given by:

$$K_{npcm} = \frac{K_{np} + 2K_{pcm} - 2(k_{pcm} - K_{np})\phi}{K_{np} + 2K_{pcm} + (k_{pcm} - K_{np})\phi} K_{pcm} + 5 \times 10^4 \beta_k \zeta \phi \rho_{pcm} c_{p,pcm} \sqrt{\frac{BT}{\rho_{np} d_{np}}} f(T, \phi) \quad (13)$$

Table 1. Properties of paraffin wax [11] and alumina [15].

Property	Paraffin wax	Al ₂ O ₃
Density (Kg/m ³)	870 at T= 300K 780 at T= 340K	3880
Specific heat (J/KgK)	2900	765
Thermal conductivity (W/mK)	0.24 at T= 300K 0.22 at T= 340K	40
Viscosity (Ns/m ²)	0.0057933	–
Latent heat (J/Kg)	190000	–
Solidus temperature (K)	331	–
Liquidus temperature (K)	331.8	–

Here B is Boltzmann constant, 1.381×10^{-23} J/K and d_{np} is the particle size of nano-material,

$$\beta_k = 8.4407 (100\phi)^{-1.07304} \quad (14)$$

and

$$f(T, \phi) = (2.8217 \times 10^{-2}\phi + 3.917 \times 10^{-3}) \frac{T}{T_{ref}} + (-3.0669 \times 10^{-2}\phi - 3.91123 \times 10^{-3})$$

where T_{ref} is the reference temperature that is 273 K.

5. Boundary Conditions and Solutions

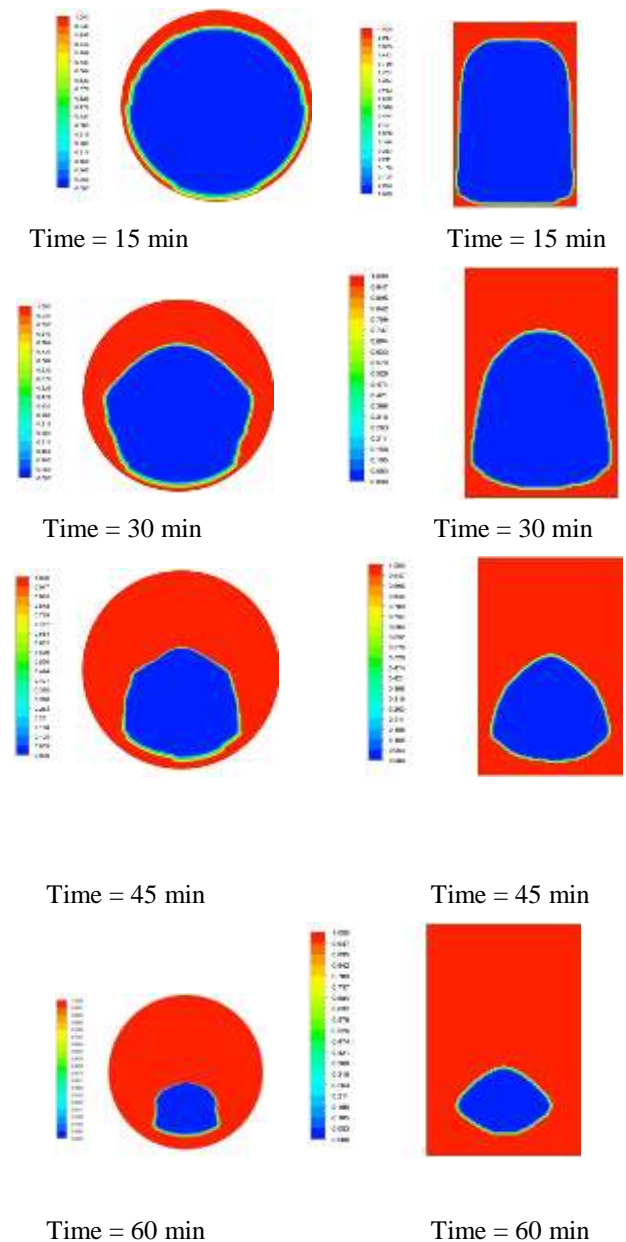
By using commercial software ANSYS 17.1 boundary conditions are provided. For the solution of momentum correction equation SECOND ORDER UPWIND scheme and for the solution of energy correction equations FIRST ORDER UPWIND scheme is invoked, whereas pressure correction equation was solved using PRESTO SCHEME. Least square cell based gradientS are employed for spatial discretization and pressure-velocity coupling is used in the solution. For pressure, momentum, and liquid fraction under relaxation factor are taken as 0.3, 0.7, and 0.4, respectively. Convergence conditions are placed down less than 10^{-5} , 10^{-8} , and 10^{-10} for continuity, momentum, and energy equation, respectively. Flow is considered to be viscous laminar, energy equation must be kept on and solidification or melting models

is registered for the set up. Materials property used for nano-enhanced PCM (nePCM) is calculated by using equations (8-14) and **Table 1**. Uniform heat flux (2500W/m^2) is registered throughout the surfaces of nano-enhanced PCM (nePCM)cavity. Standard initialization is done from all zone of the body surface, 0.1 sec time step size and 10 iterations per time step is taken for the final calculation .

Computaions are carried out for the complete melting of the PCM within a rectangular and circular cavity. Total time taken by reactangular 2-dimensional geometry is less than circular 2-dimensional geometry so it is more economic to use nano-PCM for rectangular cavity.

6. Results and Discussions

Numerical analysis of a rectangular cavity ($150 \times 100 \text{mm}$) and circular cavity (radius= 69.10mm) with supply of constant heat flux (2500W/m^2) at regular interval of 15 minutes was performed. Initially, PCM was in the solid state for that overall liquid minimum velocity zero.



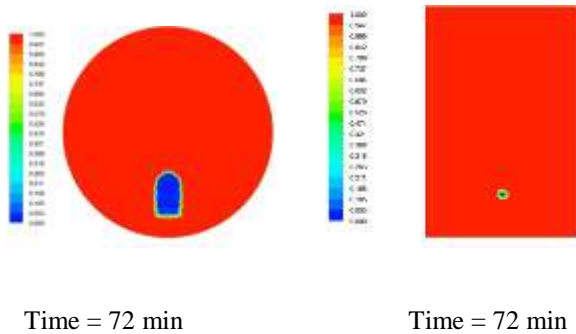


Fig. 6 Contours of liquid fraction for circular and rectangular cavity.

6.1 Contours of Liquid Fraction

Percentage of liquid fraction was noted down from 0 minute to absolute melting of the PCM solid. At the time interval of 15, 30, 45, 60, and 72 minutes liquid fraction of circular cavity was noted down as 19.499%, 45.423%, 67.594%, 85.122%, and 97.890%, respectively. Liquid fraction observed at time interval of 15, 30, 45, 60, and 72 minutes for rectangular cavity as 23.117%, 50.285%, 71.192%, 88.017%, and 99.918%, respectively. Complete melting of PCM occurred approximately at 76 minutes for circular cavity whereas 73 minutes for rectangular cavity. So there is a 2.071% improvement in the melting rate for rectangular cavity. So, it will be wise to choose the rectangular geometry for further improvement of energy storage through PCM materials.

It can be concluded from the graph shown in Fig.7 that the use of nanoparticles for rectangular cavity is better with respect to circular geometry.

6.2 Effects of addition of Al_2O_3 nanoparticles

Three different volumetric percentages (2%, 5%, and 10%) of Al_2O_3 nanoparticle is added in the rectangular cavity. By the addition of nanoparticle in PCM, the thermal conductivity of the paraffin wax is improved but latent heat of storage is decreased [10].

Table 2. Liquid fraction observed at 3600 seconds.

Process	PCM	2% nePCM	5% nePCM	10% nePCM
Melting	88.018 %	90.834 %	89.866 %	92.485 %

As it can be observed from the **Table 2** that with respect to PCM for 2%, 5%, and 10% nano-enhanced PCM (nePCM) the increase in liquid fraction was 3.199%, 2.099%, and 5.075% , respectively at 3600 sec.

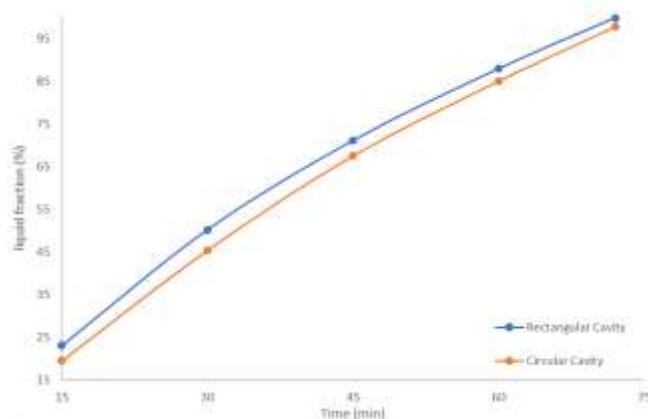


Fig. 7 Plot of liquid fraction versus time for circular and rectangular cavity.

In **Fig. 8** Transient variation of liquid fractions for base PCM and nePCM having different volume fractions in rectangular cavity is shown.

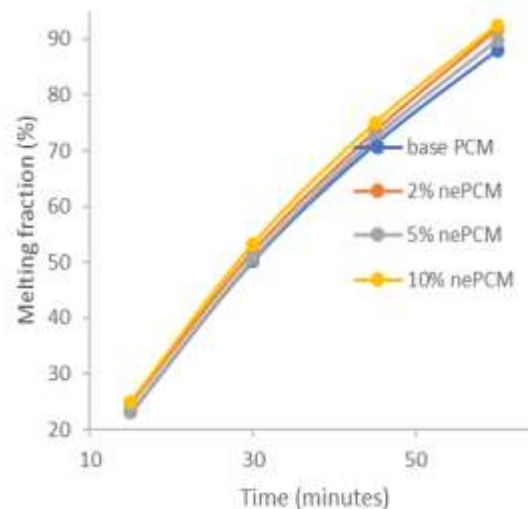


Fig. 8. Plot of liquid fraction (%) versus time (min) for different volume fractions of nePCM

Conclusions

Numerical studies employing commercial software ANSYS-FLUENT for melting process from the standpoint of energy storage was performed using two-dimensional geometries having rectangular and circular cavities with a provision for nano-enhancement where the base material was paraffin.

A grid-independence test was carried out and the results reported are essentially grid-independent. Grid-independency tests were recorded for 300s and the optimum element size obtained for rectangular mesh is 1.2mm and the optimum number of elements is 10, 500.

In this present study it reveals that with the variation of concentrations of nano-particles for a range from 2%, 5%, and 10% towards the enhancement of melting fraction, the most optimum volume fraction of nano-enhanced phase change materials is 2%.

The thermal conductivity improves and latent heat declines for nano-enhanced phase change material with reference to base material as paraffin.

For rectangular geometry 2.071% improvement in melting rate is observed in comparison to circular geometry.

2.770% enhancement in melting rate for rectangular cavity is recorded with the use of 2% nano-enhanced phase change material.

In sum, it is recommended that cavity with rectangular shape should be preferred over the circular geometry with constant heat flux boundary condition.

Data Availability Statement

All data, models, and code generated or used during the study appear in the submitted article.

Acknowledgements

The first author thankfully acknowledges the help rendered by Mr. Kundan Kumar. The first author further records her thankfulness for the financial support by Ministry of Human Resource Development (MHRD).

References

- [1] Mohamed, S. A., Al-Sulaiman, F. A., Ibrahim, N. I., Zahir, M. H., Al-Ahmed, A., Saidur, R., Yilbaş, B. S. and Sahin, A. Z., 2017. *A review on current status and challenges of inorganic phase change materials for thermal energy storage systems. Renewable and Sustainable Energy Reviews*, 70, pp. 1072-1089.
- [2] Zalba, B., Marin, J. M., Cabeza, L. F. and Mehling, H., 2003. *Review on thermal energy storage with phase change: materials, heat transfer analysis and applications. Applied thermal engineering*, 23(3), pp. 251-283.
- [3] Sharma, A., Tyagi, V. V., Chen, C. R. and Buddhi, D., 2009. *Review on thermal energy storage with phase change materials and applications. Renewable and Sustainable Energy Reviews*, 13(2), pp. 318-345.
- [4] Farid, M. M., Khudhair, A. M., Razack, S. A. K. and Al-Hallaj, S., 2004. *A review on phase change energy storage: materials and applications. Energy Conversion and Management*, 45(9-10), pp. 1597-1615.
- [5] Taylor, R. A., Chung, C. Y., Morrison, K. and Hawkes, E. R., 2014. *Analysis and testing of a portable thermal battery. Journal of Thermal Science and Engineering Applications*, 6(3).
- [6] Pielichowska, K. and Pielichowski, K., 2014. *Phase change materials for thermal energy storage. Progress in Materials Science*, 65, pp. 67-123.
- [7] Qureshi, Z. A., Ali, H. M. and Khushnood, S., 2018. *Recent advances on thermal conductivity enhancement of phase change materials for energy storage system: a review. International Journal of Heat and Mass Transfer*, 127, pp. 838-856.
- [8] Alomair, M. A., Alomair, Y. A., Abdullah, H. A., Mahmud, S. and Tasnim, S., 2017. *Nanoparticle enhanced phase change material in latent heat thermal energy storage system: an experimental study. In Proceedings of International Conference of Energy Harvest, Storage, and Transfer* (pp. 1-5).
- [9] Arasu, A. V. and Mujumdar, A. S., 2012. *Numerical study on melting of paraffin wax with Al_2O_3 in a square enclosure. International Communications in Heat and Mass Transfer*, 39(1), pp. 8-16.
- [10] Valan, A. A., Sasmito, A. P. and Mujumdar, A. S., 2013. *Numerical performance study of paraffin wax dispersed with alumina in a concentric pipe latent heat storage system. Thermal Science*, 17(2), pp. 419-430.
- [11] Vikas, A. Y. and Soni, S. K., 2017. *Simulation of Melting Process of a Phase Change Material (PCM) using ANSYS (FLUENT)*.
- [12] Dhaidan, N. S., Khodadadi, J. M., Al-Hattab, T. A. and Al-Mashat, S. M., 2013. *Experimental and numerical investigation of melting of phase change material/nanoparticle suspensions in a square container subjected to a constant heat flux. International Journal of Heat and Mass Transfer*, 66, pp. 672-683.
- [13] Huang, M. J., Eames, P. C. and Norton, B., 2007. *Comparison of predictions made using a new 3D phase change material thermal control model with experimental measurements and predictions made using a validated 2D model. Heat Transfer Engineering*, 28(1), pp.31-37.
- [14] ANSYS, A., 2016. *ANSYS FLUENT User's Guide*, 17.2. Canonsburg: ANSYS.
- [15] Yang, Y.T., Wang, Y.H. and Tseng, P.K., 2014. *Numerical optimization of heat transfer enhancement in a wavy channel using nanofluids. International Communications in Heat and Mass Transfer*, 51, pp. 9-17.
- [16] Chow, L. C., Zhong, J. K. and Beam, J. E., 1996. *Thermal conductivity enhancement for phase change storage media. International Communications in Heat and Mass Transfer*, 23(1), pp. 91-100.
- [17] Vajjha, R. S., Das, D. K. and Namburu, P. K., 2010. *Numerical study of fluid dynamic and heat transfer performance of Al_2O_3 and CuO nanofluids in the flat tubes of a radiator. International Journal of Heat and Fluid Flow*, 31(4), pp. 613-621.